Finite element simulations of nanoindentation in beta metastable Ti alloys

A.F. Gerday[1], N. Clement[2], P.J. Jacques[2], T.Pardoen[2], A.M.Habraken[1]

[1] *Department of Mechanics of materials and Structures, University of Liege (ULg)*
Chemin des Chevreuils 1, B-4000 Liege, Belgium
URL: www.ulg.ac.be/matstruc
e-mail: afgerday@ulg.ac.be; Anne.Habraken@ulg.ac.be

[2] *IMAP Department, Université Catholique de Louvain-La-Neuve (UCL)*
Place Sainte Barbe 2, B-1348 Louvain-la-Neuve, Belgium
URL: www.imap.ucl.ac.be
e-mail:clement@imap.ucl.ac.be; jacques@imap.ucl.ac.be; pardoen@imap.ucl.ac.be

ABSTRACT: Nanoindentation is a versatile tool to probe local plastic properties of materials. Finite element (FE) modelling is currently used to identify material data from nanoindentation tests [1-4]. The general ambition of this research is to extract the material parameters describing the response of a new Ti alloy, called Ti-555, in order to perform simulations on representative microscopic cells and guide the optimisation of this alloy. In this paper, the first steps of the identification of the macroscopic flow parameters of the β-phase are described. The nanoindentation tests using a pyramidal Berkovich diamond indenter are performed in the β-phase. The FEM results with different parameters of an isotropic and anisotropic elasto-plastic (EP) constitutive law are analyzed and the predicted shapes are compared to the final shape of the indented material. The FE results very much depend on physical model choices, and cannot rely on an automatic identification approach.

Key words: Nanoindentation, Ti-555, Finite Element (FE)

1 INTRODUCTION

Nanoindentation is a usual but versatile technique for material characterization. It allows evaluating basic properties, for a chosen phase, from small samples of material.
In order to identify a new generation of Ti alloy, called Ti-555 (Ti-5Al-5Mo-5V-3Cr-0.3Fe), nano-indentation tests and FE simulations are performed.
Ti-555 is a two-phase alloy involving, in general, a b.c.c. β-phase and a hexagonal α-phase. The morphology and distribution of these two phases are defined by the thermal treatments imposed to the material. Only the β-phase is taken into account in the following sections as the grains were large enough to indent only the β-phase.
First, the experimental procedure of macroscopic and microscopic tests on the Ti-555 alloy is presented. The macroscopic tensile and the nanoindentation experiments were performed at the IMAP department of the UCL.
The next section concerns the numerical approach. Simulations with the Lagamine FE code developed at the M&S department of the University of Liège [5] model the experiments. Different macroscopic phenomenological EP constitutive laws are used in order to identify the material.
The first results obtained with the FE code are analysed and compared to results obtained in the literature and by experimental tests.

2 EXPERIMENTAL PROCEDURE

Since nanoindentation simulations and tests focuse on the β-phase behaviour, a 100% β microstructure is chosen. After an appropriate heat treatment (water quenching from the high temperature β domain), the samples for nanoindentation are mechanically grinded using SiC papers down to 1200, then polished to 1 µm with diamond paste. Finally, a mechanical/chemical polishing step is carried out with an OPS colloidal suspension during 2 hours to remove the mechanically altered surface and slightly reveal the microstructure by a gentle etching.
Nanoindentation tests are performed on a Hysitron Triboscope mounted on a Park autoprobe cp AFM-STM apparatus. A three-sided Berkovich diamond tip is used with a total included angle of 142.3 degrees and a half angle of 65.35 degrees. The tip STM mode is chosen for imaging, and nanoindentation uses the capacitive transducer to record loads up to 25mN and depths up to 400 nm following the tip calibration on a fused silica reference sample. A load-displacement curve is then

obtained for each indent (figure 1).

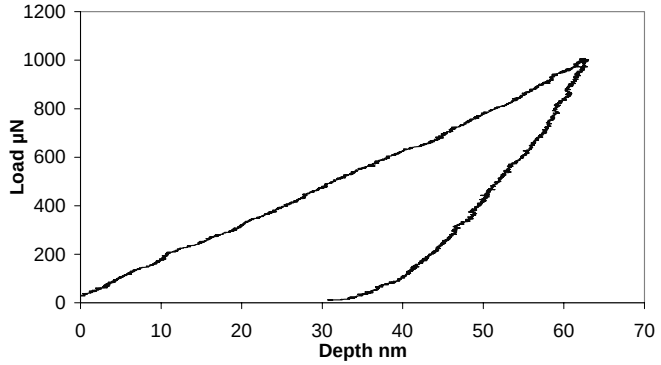

Fig.1. Nanoindentation test: load-displacement curve on Ti-555 aged 2 hours at 830°C

The only tensile data for Ti-555 (figure 2), available at this moment, was done on the raw material, with a two-phase microstructure. A strong precipitation strengthening is observed due to the fine and dispersed α precipitation in the β matrix. Micro-hardness measurements show an increase from 310 HV to 570 HV when varying the microstructure from a 100% β to a very fine α precipitation. The raw material presents an intermediate value of 434 HV, not reaching the maximum due to the coarser α precipitates. We can thus foresee that the material strength of the raw material tensile data should be decreased to render the 100% β material behaviour.

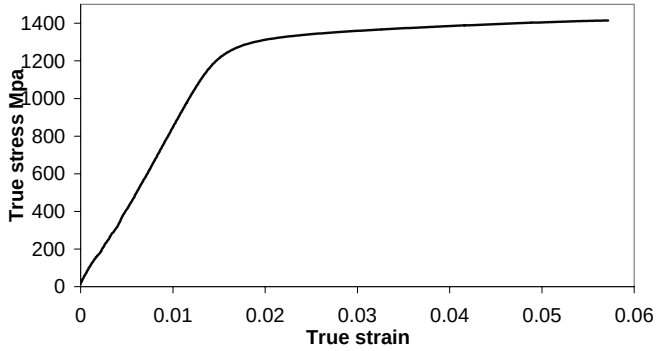

Fig.2. Tensile behaviour of the raw Ti-555

3 NUMERICAL PROCEDURE

3.1 Mesh

To model the Ti-555 specimen, 3-D FE meshes have been generated with a refined region in the contact zone. The first one is composed of 1772 eight-node brick [6] elements (mesh 1) and the second one contains 4480 elements (mesh 2). These two meshes are partly shown in figures 3.

Figures 4 give the sample dimensions (in 10^{-8} m).

Contact elements [7] with 9 integration points are put in the central zone and the indenter is considered as a rigid tool.

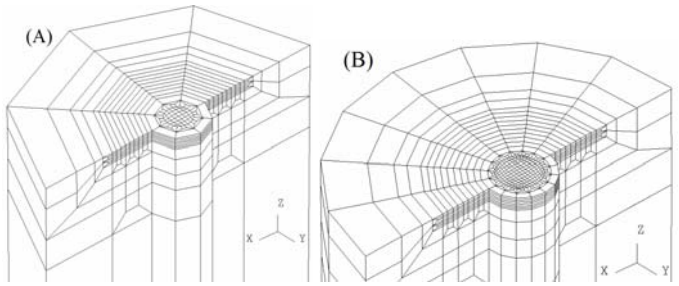

Fig.3. Parts of the meshes used, (A) mesh 1 (1772 elements) and (B) mesh 2 (4480 elements)

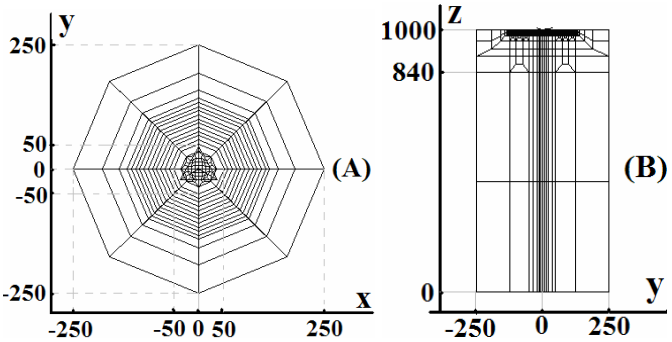

Fig.4. Mesh 1 with graduations in 10^{-8} m, (A) top view, (B) cut in the plane x = 0

3.2 Constitutive law

First, the Von Mises EP isotropic law is used to describe the material behaviour. The Young modulus is obtained from the tensile test done on a raw Ti-555 specimen and Poisson's ratio is taken to 0.36.

Then, the anisotropic Hill 1948 yield criterion is used:

$$F(\sigma_y-\sigma_z)^2+G(\sigma_z+\sigma_x)^2+H(\sigma_x+\sigma_y)^2+$$
$$2L\tau_{yz}^2+2M\tau_{zx}^2+2N\tau_{xy}^2=2\sigma_F^2$$

with σ_F the initial yield stress for a tensile test in the rolling direction. The anisotropic parameters come from the anisotropic steel grade (DC06) [8] with maximum Lankford coefficient of 2.56. This choice without link with titanium behaviour has the only goal to check the FE result sensitivity to anisotropy in nanoindentation simulations with a macroscopic phenomenological law.

The hardening parameters of the isotropic Swift hardening law

$$\sigma=K(\varepsilon_0+\varepsilon^{plast})^n$$

are obtained using the macroscopic tensile test (figure 2). The different parameters are given in table 1.

Table1. Parameters

Elasticity	Hill (DC06)	Swift (Ti-555 brut)
E = 84000 MPa	F = 0.994	K = 1583
ν = 0.36	G = 1.084	ε_0 = 4.427E-5
	H = 0.916	n = 0.0354
	N = L = M = 3.0789	

4 RESULTS

4.1 Force prediction

A first simulation of nanoindentation is done with the isotropic EP constitutive law and with the first mesh. For time = 0.8 sec, the indentation depth is 45 nm. The same simulation was also performed with the refined mesh. Figure 5 shows both FE predicted load-time curves compared to an experimental test of nanoindentation on the β-phase of the Ti-555 aged two hours at 830°C. The two numerical curves presents bumps but at different times.
In this figure, for different times, arrows show the forces applied by the indenter at the integration points of the contact elements under the tip. The central node of these meshes corresponds to the node just under the tip of the indenter. A link is present between the new integration points that enter in contact and the bumps of the curves.

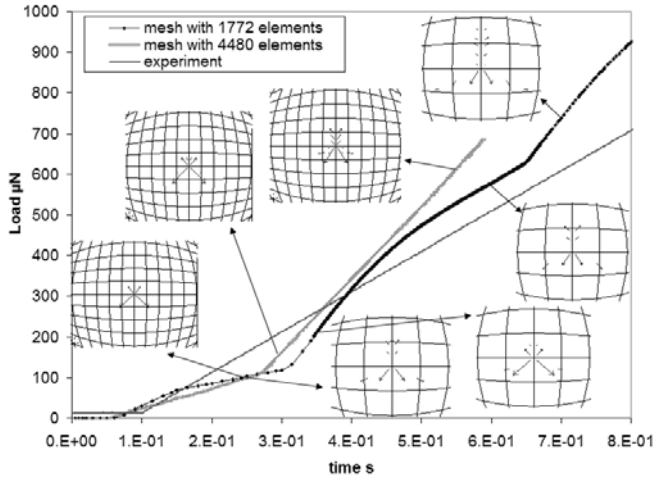

Fig.5. Nanoindentation test, experimental (in the β-phase of Ti-555 aged two hours at 830°C) and numerical load-time curves.

Differences between experiment and simulations probably come both from the identification of the parameters and from the simple constitutive law. Let us remind that the hardening law was identified from a tensile test on a raw material when the nanoindentation is performed on an aged material.

4.2 Substrate effect

The final indentation depth h is 62 nm. For this indentation, the equivalent Von Mises stress is drawn in figure 6.
At the end of the loading, the part of the sample influenced by the indenter is about 16*h. So, as mentioned in [1] and [2], the indentation depth must be less then 10 % of the height of the sample to avoid substrate effect.

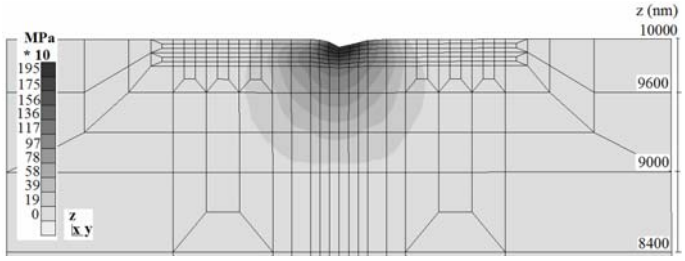

Fig.6. Von Mises equivalent stress for h = 62 nm

4.3 Effect of the material parameters on pile-up / sink-in

For materials with an identical Young modulus and identical indenter shape, Vlassak [1] predicts the apparition of pile-up around the contact area for material with a high yield stress and sink-in with lower yield stress. These conclusions were obtained for elastic-perfectly plastic materials. The results of simulations done with E = 84000 MPa, with a Berkovich tip and with a yield stress of 500 MPa and 2000 MPa are presented in figure 7 where z represents the position of the surface nodes of the sample along the cut 1, plotted in figure 8. In FE simulations, EP isotropic law without hardening is used for both simulations, in order to compare with results from [1].

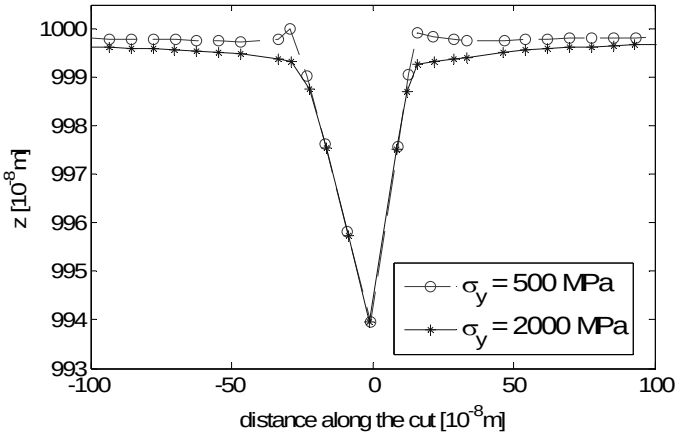

Fig.7. Nanoindentation tests. Position of the nodes at the surface of the sample in the central part along a height of the triangle tip. (Mesh 1)

As predicted, pile-up effect appears around the contact area for a small yield stress and sink-in effect is present in the other case.
The same conclusions have been obtained for simulations in which the hardening parameters were taken from table 1.

4.4 Isotropy – anisotropy

A nanoindentation simulation is done using the isotropic EP constitutive law. At the end of the simulation, corresponding to an indentation depth of 45 nm, three cuts are done along the three heights of

the tip triangle (figure 8).

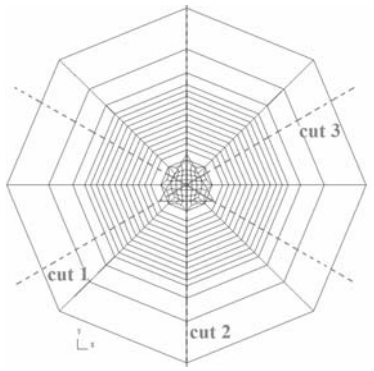

Fig.8. Cuts along the sample

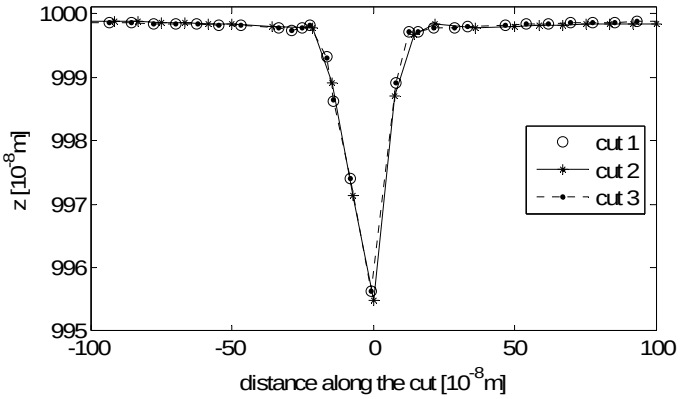

Fig.9. Nanoindentation simulation with an isotropic EP law. Position of the surface nodes along the 3 cuts of Fig.8. Mesh 1.

The results obtained and shown in figure 9 are in good agreement with the material isotropy. The curves from the first and the third cut nearly give the same results. The small differences with the second cut come from the mesh. In fact, due to the shape of the mesh, distance between two nodes for the second cut is not identical to the two other cuts.

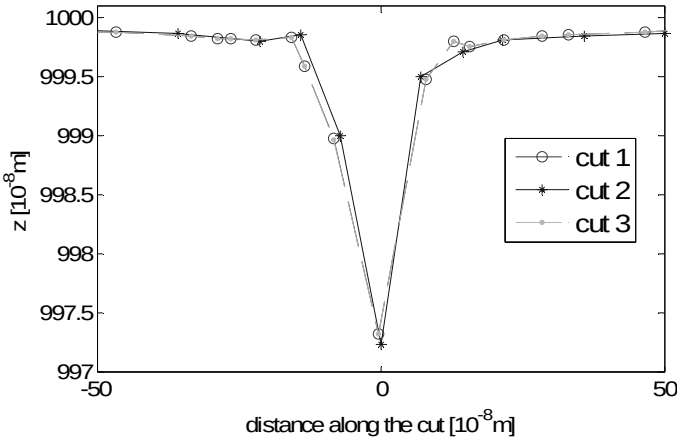

Fig.10. Nanoindentation simulation with an anisotropic EP law. Position of the surface nodes along the 3 cuts of Fig. 8.

The simulation results with the Hill parameters of table 1 and obtained after an indentation depth h = 27.6 nm are given in figure 10. The cuts show differences due to the anisotropy of the yield locus. This result confirms that nanoindentation simulations with phenomenological laws are sensitive to the constitutive law and its parameters.

5 PERSPECTIVES

Tensile tests on the aged material will be performed at different strain rate. So, both (isotropic and anisotropic) EP and EVP model will be identified on the right material. Texture measurements will be coupled with the nanoindentation tests and will help to define material anisotropy. The identification of the different active slip systems and their critical shear stress will be provided by micro tests with diffraction of neutron.

From the microscopic point of view, a microscopic crystal plasticity-based constitutive law written by Y.Huang and modified by Kysar [9] will be used to simulate the flow properties of the β-phase. The different slip systems will be supposed to be activated with identical or different critical shear stresses. Comparisons with all the experimental results will provide first identification then validation of the material data set.

REFERENCES

1. X.Chen and J.J.Vlassak, A Numerical Study on the Measurement of Thin Film Mechanical Properties by means of Nanoindentation, In: *J. Mat. Res.*, **16**(10) (2001) 2979-2982.
2. R.Saha and W.D.Nix, Effects of the substrate on the determination of thin film mechanical properties by nanoindentation, *Acta Materialia*, 50 (2002) 23-38.
3. P.L.Larsson, A.E.Giannakopoulos, E.Söderlung, D.J.Rowcliffe, R.Vestergaard, Analysis of Berkovich indentation, In: *Int. J. Solids Structures*, Vol.33, No.2, pp.221-248, 1996.
4. L.M.Farrissey, P.E.McHugh, Determination of elastic and plastic material properties using indentation: Development of method and application to a thin surface coating. *Materials Science and Engineering A*, accepted March 2005.
5. M. Dyduch, A.M. Habraken, S. Cescotto, Automatic adaptive remeshing for numerical simulations of metal forming. In: *Jl. of Comp. Meth. in Appl. Mechanics and Engineering*, 101 (1992) 283-298.
6. K.P. Li, S. Cescotto, A 8-Node Brick Element with Mixed Formulation for large deformation analyses. In: *Comp. Meth. in Appl. Mech. and Eng*., 141 (1997) 157-204.
7. A.M. Habraken & S. Cescotto, Contact between deformable solids, the fully coupled approach. *Mathematical and Computer Modelling*, 28, 4-8 (1998) 153-169.
8. P. Flores, P. Moureaux, A-M Habraken, Material Identification Using a Bi-Axial Test Machine, In: *Applied Mechanics and Materials*, 3-4 (2005) 91-98.
9. Huang Y., A user-material subroutine incorporating single crystal plasticity in the ABAQUS finite element program. *Internal report*, Harvard University, Cambridge, June 1991.